BNL-225242-2024-JAAM

GRP-COAP-62

Carbon Dioxide Insertion into Rhenium Hydrides as a Probe for the Impact of Solvent on Linear Free Energy Relationships between Thermodynamic and Kinetic Hydricity

M. R. Elsby, M. Z. Ertem

To be published in "Organometallics"

October 2023

Chemistry Department

Brookhaven National Laboratory

U.S. Department of Energy

USDOE Office of Science (SC), Basic Energy Sciences (BES)

DISCLAIMER

Carbon Dioxide Insertion into Rhenium Hydrides as a Probe for the Impact of Solvent on Linear Free Energy Relationships Between Thermodynamic and Kinetic Hydricity

Matthew R. Elsby,[a,¶] Matthew R. Espinosa,[a,¶] Mehmed Z. Ertem,[b,*] Anthony P. Deziel,[a] Nilay Hazari,[a,*] Alexander J. M. Miller,[c] Alexandra H. Paulus,[a] & Matthew V. Pecoraro[a]

[a]Department of Chemistry, Yale University, P. O. Box 208107, New Haven, Connecticut, 06520, USA. E-mail: nilay.hazari@yale.edu

[b]Chemistry Division, Brookhaven National Laboratory, Upton, New York, 11973, USA. E-mail: mzertem@bnl.gov

[c]Department of Chemistry, University of North Carolina at Chapel Hill, Chapel Hill, North Carolina, 27599, USA.

[¶]Denotes that the authors made equal contribution.

Abstract

The kinetics of CO_2 insertion into electronically different Re(^{R}bpy)(CO)$_3$H (^{R}bpy = 4,4'-R-2,2'-bipyridine; R = OMe, ^{t}Bu, Me, H, Br, COOMe, CF_3) complexes to form Re(^{R}bpy)(CO)$_3${OC(H)O} compounds were determined in acetone, dimethylacetamide (DMAc), dimethylformamide (DMF), dimethylsulfoxide (DMSO), and 3-methoxypropionitrile (3-MPN) and compared with previous data in acetonitrile (MeCN). The rates of CO_2 insertion for any one complex of the type Re(^{R}bpy)(CO)$_3$H in different solvents correlates with the Dimroth-Reichardt (E_T(30)) solvent parameter. Hammett plots in each solvent indicate that insertion reactions are faster for bpy ligands with electron-donating groups. There is, however, no correlation between the slope of the Hammett plot in different solvents and any common solvent parameter. Similarly, the enthalpies and entropies of activation and kinetic isotope effects associated with CO_2 insertion into Re(bpy)(CO)$_3$H in different solvents do not correlate with any common solvent parameters. Theoretical calculations were used to determine the relative thermodynamic hydricities of Re(^{R}bpy)(CO)$_3$H type complexes in MeCN, acetone, DMF, and DMSO and in each solvent complexes with more electron-donating substituents on the bpy ligand are stronger hydride donors. Linear Free Energy Relationships (LFERs) between calculated thermodynamic and experimental kinetic hydricity, as measured through CO_2 insertion reactions, were observed in MeCN, acetone, DMF, and DMSO. The slopes of the LFERs correlate with the dielectric constant of the solvent. Overall, this work provides fundamental information about the thermodynamics and kinetics of hydride transfer reactions in different solvents, which is valuable for catalyst design.

Introduction

Hydride transfer reactions from transition metal hydrides to organic compounds represent a crucial elementary step in many transition metal catalyzed processes.[1] For example, hydride transfer is important in transition metal catalyzed hydrogenation,[2] hydroformylation,[3] and hydrosilylation[4] reactions. Additionally, hydride transfer from a transition metal hydride to CO_2 is often a key step in the reduction of CO_2 to chemicals, such as formic acid or methanol.[5] Two quantitative parameters are often used to understand the ability of a transition metal hydride to donate a hydride to a substrate (Figure 1): i) *Thermodynamic hydricity* (ΔG^{o}_{H-}) is the free energy needed to release a hydride ion, H^-, from a transition metal hydride in solution,[6] and ii) *Kinetic hydricity* is the elementary rate constant for the transfer of a hydride to a particular substrate, which is related to $\Delta G^{\ddagger}_{H-}$.[6b,6e] Whereas thermodynamic hydricity is an intrinsic property of a transition metal hydride, kinetic hydricity varies as the substrate that is accepting the hydride is changed. Understanding thermodynamic hydricity is important because it enables predictions about whether a hydride transfer reaction is energetically favorable, while understanding kinetic hydricity is important because it enables predictions about the rate of a specific reaction.

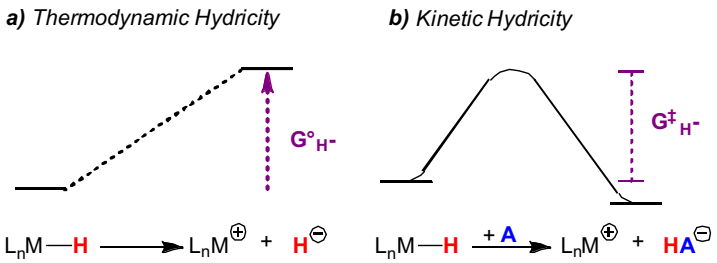

Figure 1: Representations of: **a)** Thermodynamic hydricity, which is the Gibbs free energy difference between the ground state of the metal hydride (L_nM–H) and the product of heterolytic bond scission (L_nM^+ *and* H^-). **b**) Kinetic hydricity, which is the elementary rate constant for hydride transfer from a metal hydride (L_nM–H) to a hydride acceptor (A). It varies as the acceptor is changed and is related to the free energy of activation energy ($\Delta G^{\ddagger}_{H-}$) for hydride transfer.

A challenge in using thermodynamic and/or kinetic hydricity to make predictions about transition metal catalyzed reactions is that they both vary as the solvent changes.[6e] For instance, all transition metal hydride complexes that have been measured to date have a lower thermodynamic hydricity (are more hydridic) in water than in acetonitrile (MeCN), although there is a paucity of studies in other solvents.[6e] Investigations using a structurally similar but electronically different series of complexes of the type $[Cp^*Ir(^Rbpy)H]^+$ (^Rbpy = 4,4'-R-2,2'-bipyridine; R = OMe, ^{t}Bu, Me, H, COOMe, CF_3; Cp^* = C_5Me_5), demonstrate that the complexes have the same electronic sensitivity in their thermodynamic hydricity in water and MeCN, suggesting that for this series of complexes

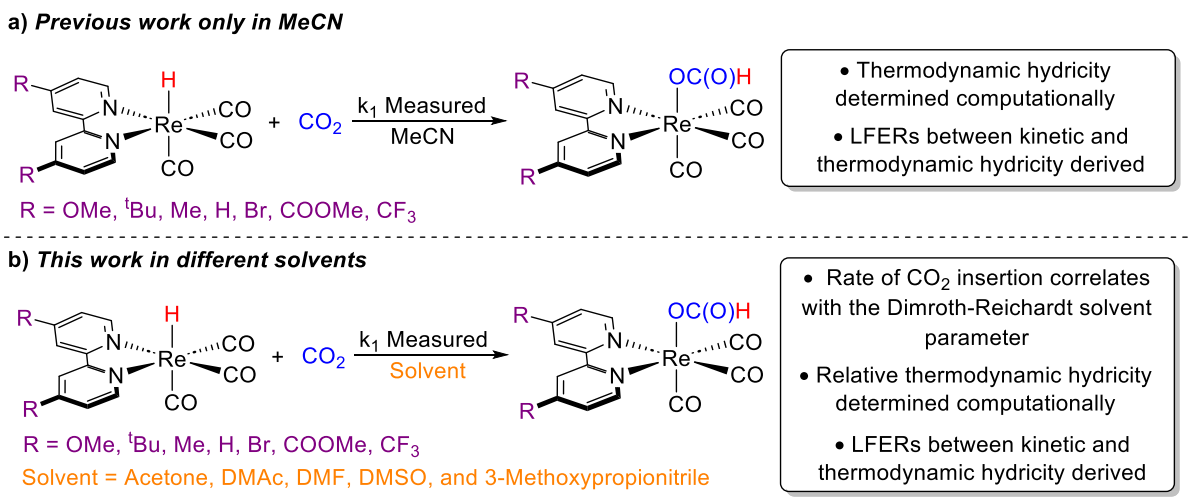

Figure 2: a) Previously correlations between kinetic and thermodynamic hydricity were determined in MeCN. **b)** In this work, kinetic and thermodynamic hydricity are correlated in different solvents.

it may be possible to translate relative thermodynamic hydricity from one solvent to the next.[7] In contrast, the relative change in thermodynamic hydricity as the solvent is varied is much larger for a gas like CO_2 compared to a typically solvated metal complex, so trends in the thermodynamic hydricity of the formate ion between solvents are quite different to those of metal complexes.[6e]

Kinetic hydricity is more easily compared across solvents than thermodynamic hydricity, which can be challenging to compare because of the need for basic thermodynamic data (*e.g.* H^+ reduction to H^-) in the solvent of interest and the fact that corrections are needed in some cases because of different thermochemical conventions in different solvents.[6e] Preliminary investigations of the influence of solvent on kinetic hydricity indicate that it is more predictable than thermodynamic hydricity. For example, recent studies on the rates of CO_2 insertion into transition metal hydrides (often a proxy for the rate of hydride transfer) indicate that the rate of insertion correlates with the Gütmann acceptor number (AN) or Dimroth-Reichardt ($E_T(30)$) parameter of the solvent.[8,9] Nevertheless, more research is required on the impact of solvent on kinetic hydricity to generalize these preliminary conclusions.

Linear free energy relationships (LFERs) that correlate a kinetic and thermodynamic parameter are often used to predict the performance of catalysts and design new systems.[10] However, it has been difficult to develop LFERs between kinetic and thermodynamic hydricity because thermodynamic and kinetic hydricity are often challenging to measure experimentally. We recently determined the kinetics of hydride transfer from $Re(^{R}bpy)(CO)_3H$ (R = OMe, ^{t}Bu, Me, H,

Br, COOMe, CF_3) to CO_2 in MeCN and computed the thermodynamic hydricities of the Re complexes using theoretical calculations (Figure 2a).[11] In MeCN, we demonstrated that there is a LFER between kinetic and thermodynamic hydricity. In this work, we experimentally determine the rates of CO_2 insertion into Re(^{R}bpy)$(CO)_3$H to form Re(^{R}bpy)$(CO)_3${OC(H)O} in five different solvents to determine kinetic hydricity (Figure 2b). This CO_2 insertion reaction is a model for the types of hydride transfer reactions from a metal hydride to CO_2 that are a crucial elementary step in thermal, electro- and photochemical systems for the catalytic reduction of CO_2 to formate.[12] We show that the rate of CO_2 insertion for any given Re complex in a solvent can be predicted by the $E_T(30)$ parameter of the solvent and that bpy ligands with electron rich substituents promote the reaction. However, there is no correlation between the slope of the Hammett plot in a solvent and any common solvent parameter. Using theoretical calculations, we determined the relative thermodynamic hydricity of complexes of the type Re(^{R}bpy)$(CO)_3$H in acetone, DMF, and DMSO in addition to MeCN. In each solvent, complexes with more electron-donating substituents on the bpy ligand are stronger hydride donors Finally, we show that LFERs exist between kinetic and thermodynamic hydricity in different solvents and the slopes of the LFERs correlate with the dielectric constant of the solvent, which is likely to be useful for the design of improved catalysts.

Results and Discussion

Experimental Measurements of Kinetic Hydricity

The rate of CO_2 insertion into Re hydrides of the form Re(^{R}bpy)$(CO)_3$H to generate Re(^{R}bpy)$(CO)_3${OC(H)O} is an indicator of the kinetic hydricity of the Re complexes[11] because the first step in these reactions is the rate-determining outer-sphere hydride transfer[13] to CO_2 (Figure 3). To understand the impact of solvent on the rates of CO_2 insertion into our family of Re complexes, we measured the kinetics of insertion in acetone, dimethylacetamide (DMAc), dimethylformamide (DMF), dimethylsulfoxide (DMSO), and 3-methoxypropionitrile (3-MPN) to complement our previous data in MeCN (Figure 2b).[11,14] As observed previously, these reactions

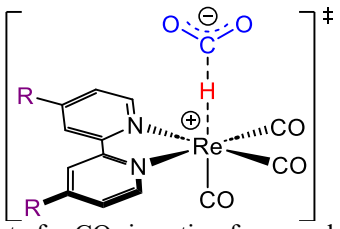

Figure 3: Rate determining transition state for CO_2 insertion for complexes of the type Re(^{R}bpy)$(CO)_3$H.[11] This type of transition state is consistent with rate limiting hydride transfer and thus the rate of the reaction is a measure of the kinetic hydricity of the complex.

are first-order in [Re] and [CO_2], with an overall rate law of rate = k_1[Re(^{R}bpy)$(CO)_3$H][CO_2] (see SI).[11,15] Values of k_1 for each reaction were obtained by dividing the k_{obs} value (from a plot of ln([Re(^{R}bpy)$(CO)_3$H] versus time) by the concentration of CO_2. The concentration of CO_2 in different solvents was determined using quantitative $^{13}C\{^1H\}$ NMR spectroscopy (see SI).

We observe a very strong correlation between the rate constant for CO_2 insertion into any single Re complex (for example Re(bpy)$(CO)_3$H or Re(^{CF3}bpy)$(CO)_3$H) and the $E_T(30)$ parameter of the solvent (Figure 4). This indicates that for a given Re complex, the rate of CO_2 insertion in different solvents can be predicted based on the solvent $E_T(30)$ parameter. In contrast, to the clear correlation with $E_T(30)$, the correlation with solvent dielectric constant and the rate of CO_2 insertion is poor (see Figures S15-S21), while the correlation with AN is good but not as strong as $E_T(30)$ (see Figures S8-S14). Our results are consistent with previous observations about the relationship between the rates of CO_2 insertion and solvent properties for metal hydride, hydroxide, and alkyl species and demonstrate that the correlation with $E_T(30)$ is likely more general than initially proposed.[8,16]

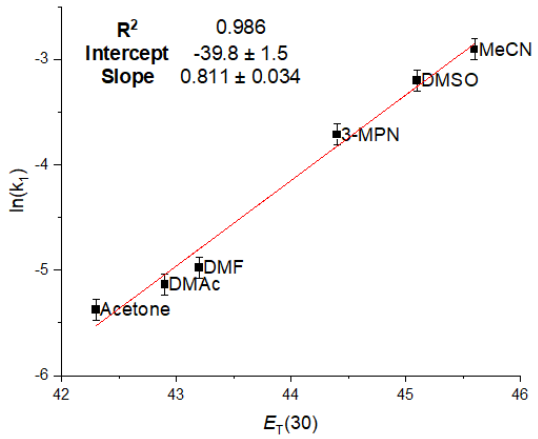

Figure 4: Plot of the rate of CO_2 insertion into Re(bpy)$(CO)_3$H against $E_T(30)$. The same trends are observed for other substituted bpy complexes (see Figures S2-S7).

We constructed Hammett plots for CO_2 insertion into Re(^{R}bpy)$(CO)_3$H in acetone, DMAc, DMF, DMSO, and 3-MPN. A representative Hammett plot in acetone is shown in Figure 5, with other data in the SI. We use a summed Hammett parameter ($\Sigma\sigma_p$) because there are two substituents on the bpy ligand and $\Sigma\sigma_p$ gives a better fit than either $\Sigma\sigma_p^+$ or $\Sigma\sigma_p^-$ (see SI).[17] In all cases the slopes of the Hammett plot are negative, indicating that electron-donating substituents on the bpy ligand promote CO_2 insertion. Given the transition state proposed in Figure 3, this is not surprising, as

a)

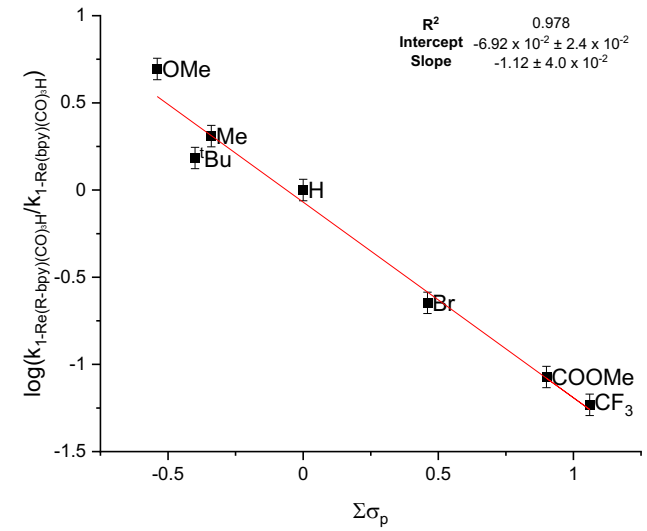

b)

Solvent	Slope of Hammett Plot (ρ)
MeCN[a]	-1.19
Acetone	-1.12
DMAc	-1.06
DMF	-0.90
DMSO	-1.37
3-MPN	-2.34

[a]From reference 11.

Figure 5: a) Representative Hammett plot for CO_2 insertion into Re(^{R}bpy)$(CO)_3H$ in acetone. **b)** Slopes of Hammett plots in different solvents.

the electron-donating substituents should stabilize the increasing positive charge on the Re center in the transition state. Our results are consistent with prior studies exploring the effect of the ancillary ligand on CO_2 insertion reactions.[8a,11] The slopes of the Hammett plot vary significantly across the solvent series, with the largest ρ value being 2.6-fold greater than the smallest value. However, analysis of the slopes of the Hammett plots in different solvent reveals no trends based on any common solvent parameter, for example dielectric constant or $E_T(30)$. It is also surprising that the slope of the Hammett plot in 3-MPN is considerably more negative than any other solvent, especially given the presumed similarities between 3-MPN and MeCN. The lack of identifiable dependence of the slope of the Hammett plot on the properties of the solvent suggests that the magnitude of electronic effects on the kinetics of CO_2 insertion are not impacted by solvent in a predictable fashion.

To gain further information about the effect of solvent on CO_2 insertion, we performed Eyring analysis of CO_2 insertion reactions into the unsubstituted complex Re(bpy)$(CO)_3H$ in different solvents (Table 1). Although negative entropies were found for insertion in all solvents, indicating a highly organized rate-limiting transition state, there were large differences between the solvents. For example, the transition state is entropically unfavorable by -19.40 cal mol^{-1} K^{-1} in 3-MPN, compared to -40.10 cal mol^{-1} K^{-1} in MeCN. This large difference between 3-MPN and MeCN is consistent with the differences in the ρ values between 3-MPN and MeCN and may suggest that for these solvents there is a correlation between solvent ordering and steepness of the Hammett

Table 1: Activation parameters and kinetic isotope effect values for CO_2 insertion into $Re(bpy)(CO)_3H$ in different solvents.

Solvent	$\Delta H^{\ddagger}$ (kcal mol^{-1})	$\Delta S^{\ddagger}$ (cal mol^{-1} K^{-1})	$\Delta G^{\ddagger}_{303}$ (kcal mol^{-1})	KIE (k_H/k_D)
Acetonitrile[a]	7.4 ± 0.7	-40.1 ± 4.0	19.6 ± 1.9	0.60 ± 0.08
Acetone	11.0 ± 1.1	-32.4 ± 3.2	20.8 ± 2.1	0.61 ± 0.09
DMAC	13.7 ± 1.3	-23.7 ± 2.3	20.8 ± 2.1	0.31 ± 0.04
DMF	11.5 ± 1.1	-30.9 ± 3.0	20.8 ± 2.1	0.37 ± 0.05
DMSO	12.7 ± 1.2	-22.4 ± 2.2	19.5 ± 1.9	0.41 ± 0.06
3-MPN	13.9 ± 1.3	-19.4 ± 1.9	19.8 ± 1.9	0.36 ± 0.05

[a]From reference 11.

slope. In general, there appears to be an offsetting effect between $\Delta H^{\ddagger}$ and $\Delta S^{\ddagger}$ and solvents that have a low $\Delta H^{\ddagger}$ have a more negative $\Delta S^{\ddagger}$. For instance, $\Delta H^{\ddagger}$ is 7.40 kcal mol^{-1} in MeCN, but 13.90 kcal mol^{-1} in 3-MPN. Within the error of our measurements $\Delta G^{\ddagger}_{303}$ is similar across all the solvents, consistent with the relatively similar rate constants in different solvents (a factor of 20 difference). Nevertheless, the origins for the significant differences in enthalpy and entropy between different solvents are unclear, although similar differences have been observed in the literature, without an explanation.[8] We also determined the kinetic isotope effects (KIEs), k_H/k_D, for CO_2 insertion into $Re(bpy)(CO)_3H$ and $Re(bpy)(CO)_3D$. An inverse KIE is observed in all solvents, which is expected because the strength of the C–H bond formed is greater than the strength of the M–H bond broken.[8b,11,15] However, the KIEs range from 0.36-0.60, and at this stage we do not have an explanation for this difference. The magnitude of the KIE does not correlate with any solvent parameter and there is also no correlation between $\Delta H^{\ddagger}$ or $\Delta S^{\ddagger}$ and the measured KIE.

Computational Estimation of Relative Thermodynamic Hydricity and Linear Free Energy Relationships

In previous work we found that it is challenging to experimentally measure the thermodynamic hydricity of complexes of the form $Re(^{R}bpy)(CO)_3H$ because of problems with their solution stability.[11] Therefore, to determine the thermodynamic hydricity of our family of $Re(^{R}bpy)(CO)_3H$ complexes in different solvents, we turned to computational approaches and performed theoretical calculations (see computational methods in SI). A common method for calculating the thermodynamic hydricity of a complex is to take the average of computed thermodynamic hydricities from isodesmic equilibrium exchange reactions between the compound of interest and other transition metal hydride acceptors with known experimental thermodynamic affinities.[6e] In

Table 2: Computed relative thermodynamic hydricities of Re(^{R}bpy)(CO)$_3$H in different solvents, determined through isodesmic exchange reactions with Re(bpy)(CO)$_3$(solvent)$^+$.[a]

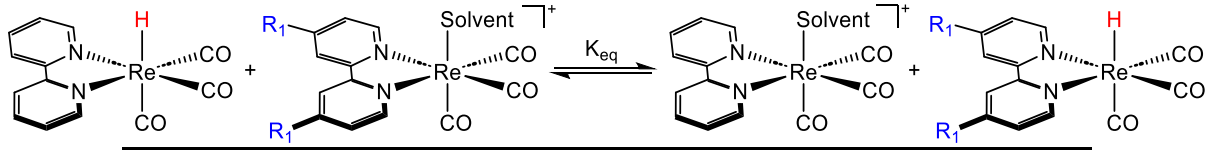

Complex	Relative Thermodynamic Hydricity (kcal mol^{-1})			
	MeCN	***Acetone***	***DMF***	***DMSO***
Re(^{OMe}bpy)(CO)$_3$H	-0.9	-1.2	-0.9	-0.8
Re(^{tBu}bpy)(CO)$_3$H	-0.4	-0.5	-0.3	-0.3
Re(^{Me}bpy)(CO)$_3$H	-0.5	-0.6	-0.5	-0.5
Re(bpy)(CO)$_3$H	0.0	0.0	0.0	0.0
Re(^{Br}bpy)(CO)$_3$H	1.1	1.2	1.0	1.1
Re(^{COOMe}bpy)(CO)$_3$H	0.9	1.1	1.2	1.0
Re(^{CF_3}bpy)(CO)$_3$H	1.7	1.9	1.6	1.7

[a]All computations were performed at the M06/def2-TZVP level with SMD continuum solvation model for the appropriate solvent using optimized structures at the B3LYP-D3 level of theory.

our case, there are almost no experimental determinations of thermodynamic hydricity in solvents such as acetone or DMF, which means that this type of approach cannot be used.[6e] Consequently, we estimated relative thermodynamic hydricity, which is sufficient for the purpose of developing LFERs, through isodesmic exchange reactions between Re(^{R}bpy)(CO)$_3$H and Re(bpy)(CO)$_3$(solvent)$^+$ in MeCN, acetone, DMF, and DMSO (Table 2).[18] We tested different density functionals and observed strong correlations between calculated thermodynamic and experimental kinetic hydricities despite differences in slopes (Tables S11-S15 and Figures S32-S36). Here, we limit our discussion to computed relative hydricities obtained at the M06 level of theory[19] in conjunction with SMD continuum solvation model[20] on optimized structures at the B3LYP-D3 level of theory[21] in vacuum (see SI for further details). A limitation of this approach is that continuum solvation models are not available for all solvents (*e.g.*, 3-MPN) so we focused on MeCN, acetone, DMF, and DMSO.

The data in Table 2 indicates that complexes with electron-donating substituents on the bpy ligand are stronger hydride donors in all solvents, while complexes with electron-withdrawing substituents on the bpy ligand are weaker donors. Additionally, the span between the weakest and strongest hydride donor is similar across all solvents (the range is 2.6-3.1 kcal mol^{-1}), which indicates that as observed for [Cp*Ir(^{R}bpy)H]$^+$ in MeCN and water,[7] the complexes have the same electronic sensitivity in their thermodynamic hydricity across a range of solvents. This suggests that for transition metal complexes it may be possible to determine the sensitivity to electronic 6

changes in thermodynamic hydricity in one solvent, and then extrapolate it to other solvents without performing more experiments.

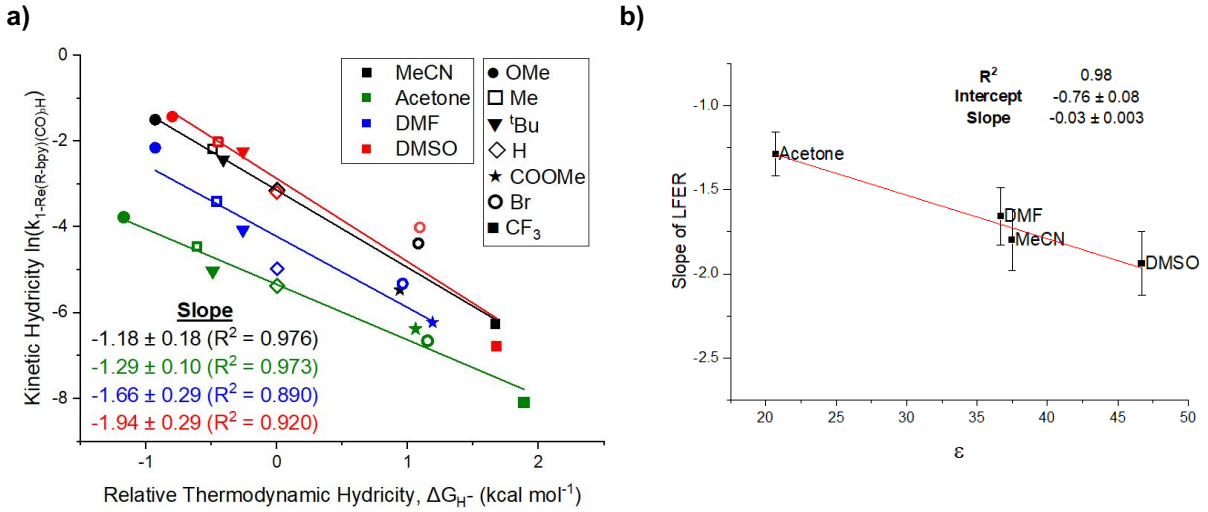

Figure 6: a) LFERs between relative thermodynamic hydricity and kinetic hydricity (determined using the rate constants for CO_2 insertion) for Re(^{R}bpy)$(CO)_3$H in MeCN (black), acetone (pink), DMF (blue), and DMSO (red); **b)** Relationship between the slopes of LFERs correlating relative thermodynamic hydricity and kinetic hydricity in different solvents and the dielectric constant of the solvent.

Using the computed relative thermodynamic hydricities for Re(^{R}bpy)$(CO)_3$H we examined the relationship between relative thermodynamic hydricity and the experimental rates of CO_2 insertion in acetone, DMF, DMSO, and MeCN (Figure 6a). In all cases, LFERs are observed between relative thermodynamic hydricity and kinetic hydricity, with more thermodynamically hydridic donors giving faster rates of insertion. The quality of the correlation varies slightly across the different solvents, but the trends are clear and strongly suggest that LFERs between kinetic and thermodynamic hydricity exist across different solvents. This is the first time that it has been demonstrated that LFERs between kinetic and thermodynamic hydricity extend across different solvents.

A feature of the LFERs in different solvents is that the slopes correlate well with the dielectric constant of the solvent (and reasonably well with the $E_T(30)$ value, Figure S37), albeit we only have four data points at this stage (Figure 6b). Solvents with higher dielectric constants, such as MeCN, give shallower slopes in the LFER, and the difference between kinetic and thermodynamic effects is most pronounced in solvents with lower dielectric constants. In the case of the CO_2 insertion reactions studied here, this may be related to the zwitterionic nature of the transition state (Figure 3), which leads to a large solvent influence in less polar solvents, where the solvent is less

able to assist in stabilizing the transition state. In contrast, it is possible that in hydride transfer reactions that involve less build-up of charge in the transition state, the impact of solvent on the LFERs will be smaller. Our results also suggest that in catalytic reactions involving CO_2 insertion, it is likely possible to achieve higher rates of CO_2 insertion by changing solvent, while maintaining similar thermodynamic driving forces. This is important because in many CO_2 reduction reactions, CO_2 insertion into a metal hydride competes with protonation of a metal hydride to generate H_2,[22] and making CO_2 insertion more thermodynamically favorable will also result in an increase in the thermodynamics of protonation. Hence, if changing the solvent results in a greater impact in the kinetics of CO_2 insertion relative to protonation, this will be a strategy for improving selectivity. To assess if this is possible, future work that explores the effect of solvents on LFERs for hydride transfer, which include a wider range of hydride acceptors than just CO_2 are required.

Conclusions

In this work, we have explored the effect of solvent on the rates of CO_2 insertion into complexes of the type Re(^{R}bpy)$(CO)_3$H, which is a direct measure of kinetic hydricity in different solvents. Our results provide strong support to several proposals in the literature relating to CO_2 insertion reactions such as: (i) more electron-donating ancillary ligands promote CO_2 insertion,[8a,15] (ii) the rates of insertion into a given complex in different solvents correlate with the solvent $E_T(30)$ value,[8,16] and (iii) inverse KIEs are observed for insertion into a metal hydride compared to a metal deuteride.[8,11,15] However, based on our current level of understanding we are unable to explain how Hammett parameters, activation enthalpies and entropies, and KIEs for CO_2 insertion into metal hydrides vary as the solvent is changed. For the development and optimization of catalysts, the most important feature of our work is likely that electronic trends on CO_2 insertion in one solvent are broadly the same in a different solvent, with more electron-donating ligands promoting insertion reactions, although the magnitude of electronic effects varies between solvents.

We used theoretical calculations to determine the relative thermodynamic hydricity of complexes of the type Re(^{R}bpy)$(CO)_3$H and in all solvents complexes with electron-donating substituents on the bpy are more powerful hydride donors. Our results suggest that electronic effects on thermodynamic hydricity do not differ markedly between solvents, which broadens previous work[6e] to a wider range of solvents. Using our experimental values of kinetic hydricity and calculated relative thermodynamic hydricities, we extended our recent work in MeCN,[11] and

showed for the first time that LFERs between kinetic and thermodynamic hydricity exist in different solvents and the slopes of the trendlines of the LFERs in different solvents correlate strongly with the dielectric constant of the solvents. Overall, this work provides fundamental information about the impact of solvent on hydride transfer reactions, which is likely to be relevant to designing improved catalysts given the plethora of transformations that involve hydride transfer.

Acknowledgements

NH acknowledges support from the National Science Foundation through Grant CHE-1953708 and the Yale Center for Natural Carbon Capture. MRE (Elsby) acknowledges the support of the Natural Sciences and Engineering Research Council of Canada (NSERC), PDF-568014-2022. The work at Brookhaven National Laboratory (MZE) was carried out under contract DE-SC0012704 with the U.S. Department of Energy, Office of Science, Office of Basic Energy Sciences, and utilized computational resources at the Center for Functional Nanomaterials, which is a U.S. Department of Energy Office of Science Facility, and the Scientific Data and Computing Center, a component of the Computational Science Initiative, at Brookhaven National Laboratory under Contract No. DE-SC0012704. Conceptual aspects of thermodynamic hydricity and solvent correlations were supported by the U.S. Department of Energy, Office of Science, Office of Basic Energy Sciences, under Award No. DE-SC0014255 (AJMM).

Supporting Information

Details about selected experiments, kinetics data, computational information, Cartesian coordinates and energies of the optimized geometries.

Competing Financial Interests

The authors declare no competing financial interests.

References

1. (a) Samec, J. S.; Bäckvall, J.-E.; Andersson, P. G.; Brandt, P. Mechanistic Aspects of Transition Metal-Catalyzed Hydrogen Transfer Reactions. *Chem. Soc. Rev.* **2006**, *35*, 237-248; (b) Larionov, E.; Li, H.; Mazet, C. Well-Defined Transition Metal Hydrides in Catalytic Isomerizations. *Chem. Commun.* **2014**, *50*, 9816-9826; (c) Ai, W.; Zhong, R.; Liu, X.; Liu, Q. Hydride Transfer Reactions Catalyzed by Cobalt Complexes. *Chem. Rev.* **2018**, *119*, 2876-2953.
2. (a) Bäckvall, J.-E. Transition Metal Hydrides as Active Intermediates in Hydrogen Transfer Reactions. *J. Organomet. Chem.* **2002**, *652*, 105-111; (b) Blaser, H.-U.; Malan, C.; Pugin, B.; Spindler, F.; Steiner, H.; Studer, M. Selective Hydrogenation for Fine Chemicals: Recent Trends and New Developments. *Adv. Synth. Catal.* **2003**, *345*, 103-151; (c) Clapham, S. E.; Hadzovic, A.; Morris, R. H. Mechanisms of the H_2-Hydrogenation and Transfer Hydrogenation of Polar Bonds Catalyzed by Ruthenium Hydride Complexes. *Coord. Chem. Rev.* **2004**, *248*, 2201-2237; (d) Johnson, N. B.; Lennon, I. C.; Moran, P. H.; Ramsden, J. A. Industrial-Scale Synthesis and Applications of Asymmetric Hydrogenation Catalysts. *Acc. Chem. Res.* **2007**, *40*, 1291-1299; (e) Wang, D.; Astruc, D. The Golden

Age of Transfer Hydrogenation. *Chem. Rev.* **2015**, *115*, 6621-6686; (f) Seo, C. S. G.; Morris, R. H. Catalytic Homogeneous Asymmetric Hydrogenation: Successes and Opportunities. *Organometallics* **2019**, *38*, 47-65; (g) Baidilov, D.; Hayrapetyan, D.; Khalimon, A. Y. Recent Advances in Homogeneous Base-Metal-Catalyzed Transfer Hydrogenation Reactions. *Tetrahedron* **2021**, *98*, 132435.

3. (a) Hilt, G. Double Bond Isomerisation and Migration—New Playgrounds for Transition Metal-Catalysis. *ChemCatChem* **2014**, *6*, 2484-2485; (b) Larionov, E.; Li, H.; Mazet, C. Well-Defined Transition Metal Hydrides in Catalytic Isomerizations. *Chem. Commun.* **2014**, *50*, 9816-9826; (c) Hassam, M.; Taher, A.; Arnott, G. E.; Green, I. R.; van Otterlo, W. A. L. Isomerization of Allylbenzenes. *Chem. Rev.* **2015**, *115*, 5462-5569; (d) Vasseur, A.; Bruffaerts, J.; Marek, I. Remote Functionalization Through Alkene Isomerization. *Nature Chem.* **2016**, *8*, 209-219; (e) Massad, I.; Marek, I. Alkene Isomerization through Allylmetals as a Strategic Tool in Stereoselective Synthesis. *ACS Catal.* **2020**, *10*, 5793-5804; (f) Fiorito, D.; Scaringi, S.; Mazet, C. Transition Metal-Catalyzed Alkene Isomerization as an Enabling Technology in Tandem, Sequential and Domino Processes. *Chem. Soc. Rev.* **2021**, *50*, 1391-1406.

4. (a) Franke, R.; Selent, D.; Börner, A. Applied Hydroformylation. *Chem. Rev.* **2012**, *112*, 5675-5732; (b) Wu, X.-F.; Fang, X.; Wu, L.; Jackstell, R.; Neumann, H.; Beller, M. Transition-Metal-Catalyzed Carbonylation Reactions of Olefins and Alkynes: A Personal Account. *Acc. Chem. Res.* **2014**, *47*, 1041-1053; (c) Clarke, M. L. Hydroformylation. Fundamentals, Processes, and Applications in Organic Synthesis. By Armin Börner and Robert Franke. *Angew. Chem. Int. Ed.* **2016**, *55*, 13377-13377; (d) Nurttila, S. S.; Linnebank, P. R.; Krachko, T.; Reek, J. N. H. Supramolecular Approaches To Control Activity and Selectivity in Hydroformylation Catalysis. *ACS Catal.* **2018**, *8*, 3469-3488; (e) Chakrabortty, S.; Almasalma, A. A.; de Vries, J. G. Recent Developments in Asymmetric Hydroformylation. *Catal. Sci. Technol.* **2021**, *11*, 5388-5411; (f) Rodrigues, F. M. S.; Carrilho, R. M. B.; Pereira, M. M. Reusable Catalysts for Hydroformylation-Based Reactions. *Eur. J. Inorg. Chem.* **2021**, *2021*, 2294-2324.

5. (a) Cokoja, M.; Bruckmeier, C.; Rieger, B.; Herrmann, W. A.; Kühn, F. E. Transformation of Carbon Dioxide with Homogeneous Transition-Metal Catalysts: A Molecular Solution to a Global Challenge? *Angew. Chem. Int. Ed.* **2011**, *50*, 8510-8537; (b) Goeppert, A.; Czaun, M.; Jones, J.-P.; Surya Prakash, G. K.; Olah, G. A. Recycling of Carbon Dioxide to Methanol and Derived Products – Closing the Loop. *Chem. Soc. Rev.* **2014**, *43*, 7995-8048; (c) Li, Y.-N.; Ma, R.; He, L.-N.; Diao, Z.-F. Homogeneous Hydrogenation of Carbon Dioxide to Methanol. *Catal. Sci. Technol.* **2014**, *4*, 1498-1512; (d) Wang, W.-H.; Himeda, Y.; Muckerman, J. T.; Manbeck, G. F.; Fujita, E. CO_2 Hydrogenation to Formate and Methanol as an Alternative to Photo- and Electrochemical CO_2 Reduction. *Chem. Rev.* **2015**, *115*, 12936-12973; (e) Klankermayer, J.; Wesselbaum, S.; Beydoun, K.; Leitner, W. Selective Catalytic Synthesis Using the Combination of Carbon Dioxide and Hydrogen: Catalytic Chess at the Interface of Energy and Chemistry. *Angew. Chem. Int. Ed.* **2016**, *55*, 7296-7343; (f) Bernskoetter, W. H.; Hazari, N. Reversible Hydrogenation of Carbon Dioxide to Formic Acid and Methanol: Lewis Acid Enhancement of Base Metal Catalysts. *Acc. Chem. Res.* **2017**, *50*, 1049-1058; (g) Sordakis, K.; Tang, C.; Vogt, L. K.; Junge, H.; Dyson, P. J.; Beller, M.; Laurenczy, G. Homogeneous Catalysis for Sustainable Hydrogen Storage in Formic Acid and Alcohols. *Chem. Rev.* **2018**, *118*, 372-433.

6. (a) McSkimming, A.; Colbran, S. B. The Coordination Chemistry of Organo-Hydride Donors: New Prospects for Efficient Multi-Electron Reduction. *Chem. Soc. Rev.* **2013**, *42*, 5439-5488; (b) Wiedner, E. S.; Chambers, M. B.; Pitman, C. L.; Bullock, R. M.; Miller, A. J. M.; Appel, A. M. Thermodynamic Hydricity of Transition Metal Hydrides. *Chem. Rev.* **2016**, *116*, 8655-8692; (c) Ilic, S.; Alherz, A.; Musgrave, C. B.; Glusac, K. D. Thermodynamic and Kinetic Hydricities of Metal-Free Hydrides. *Chem. Soc. Rev.* **2018**, *47*, 2809-2836; (d) Waldie, K. M.; Ostericher, A. L.; Reineke, M. H.; Sasayama, A. F.; Kubiak, C. P. Hydricity of Transition-Metal Hydrides: Thermodynamic Considerations for CO_2 Reduction. *ACS Catal.* **2018**, *8*, 1313-1324; (e) Brereton, K. R.; Smith, N. E.; Hazari, N.; Miller, A. J. M. Thermodynamic and Kinetic Hydricity of Transition Metal Hydrides. *Chem. Soc. Rev.* **2020**, *49*, 7929-7948.

7. Brereton, K. R.; Jadrich, C. N.; Stratakes, B. M.; Miller, A. J. M. Thermodynamic Hydricity Across Solvents: Subtle Electronic Effects and Striking Ligation Effects in Iridium Hydrides. *Organometallics* **2019**, *38*, 3104-3110.

8. (a) Heimann, J. E.; Bernskoetter, W. H.; Hazari, N.; Mayer, J. M. Acceleration of CO_2 Insertion into Metal Hydrides: Ligand, Lewis Acid, and Solvent Effects on Reaction Kinetics. *Chem. Sci.* **2018**, *9*, 6629-6638; (b) Heimann, J. E.; Bernskoetter, W. H.; Hazari, N. Understanding the Individual and Combined Effects of Solvent and Lewis Acid on CO_2 Insertion into a Metal Hydride. *J. Am. Chem. Soc.* **2019**, *141*, 10520-10529.

9. The Dimroth-Reichardt $E_T(30)$ parameter is approximately related to solvent polarity and is determined from the molar electronic transition energy of 2,6-diphenyl-4-(2,4,6-triphenylpyridinium-1-yl)phenolate (conventionally referred to as Betaine 30). It is found by measuring the λ_{max} of Betaine 30 in a particular solvent and a smaller λ_{max} corresponds to a larger wavenumber and therefore a more polar solvent. For more information see: (a) Reichardt, C. Empirical Parameters of the Polarity of Solvents. *Angew. Chem. Int. Ed.* **1965**, *4*, 29-40; (b) Reichardt, C. Solvatochromic Dyes as Solvent Polarity Indicators. *Chem. Rev.* **1994**, *94*, 2319-2358.

10. (a) Mochida, I.; Yoneda, Y. Linear Free Energy Relationships in Heterogeneous Catalysis: I. Dealkylation of Alkylbenzenes on Cracking Catalysts. *J. Catal.* **1967**, *7*, 386-392; (b) Bjelic, S.; Åqvist, J. Catalysis and Linear Free Energy Relationships in Aspartic Proteases. *Biochemistry* **2006**, *45*, 7709-7723; (c) Miller, J. J.; Sigman, M. S. Quantitatively Correlating the Effect of Ligand-Substituent Size in Asymmetric Catalysis Using Linear Free Energy Relationships. *Angew. Chem. Int. Ed.* **2008**, *47*, 771-774; (d) Pothupitiya, J. U.; Hewawasam, R. S.; Kiesewetter, M. K. Urea and Thiourea H-Bond Donating Catalysts for Ring-Opening Polymerization: Mechanistic Insights via (non) Linear Free Energy Relationships. *Macromolecules* **2018**, *51*, 3203-3211; (e) Lan, Z.; Sharada, S. M. A Framework for Constructing Linear Free Energy Relationships to Design Molecular Transition Metal Catalysts. *Phys. Chem. Chem. Phys.* **2021**, *23*, 15543-15556.
11. Espinosa, M. R.; Ertem, M. Z.; Barakat, M.; Bruch, Q. J.; Deziel, A. P.; Elsby, M. R.; Hasanayn, F.; Hazari, N.; Miller, A. J.; Pecoraro, M. V. Correlating Thermodynamic and Kinetic Hydricities of Rhenium Hydrides. *J. Am. Chem. Soc.* **2022**, *144*, 17939-17954.
12. (a) Schmeier, T. J.; Dobereiner, G. E.; Crabtree, R. H.; Hazari, N. Secondary Coordination Sphere Interactions Facilitate the Insertion Step in an Iridium(III) CO_2 Reduction Catalyst. *J. Am. Chem. Soc.* **2011**, *133*, 9274-9277; (b) Langer, R.; Diskin-Posner, Y.; Leitus, G.; Shimon, L. J. W.; Ben-David, Y.; Milstein, D. Low-Pressure Hydrogenation of Carbon Dioxide Catalyzed by an Iron Pincer Complex Exhibiting Noble Metal Activity. *Angew. Chem. Int. Ed.* **2011**, *50*, 9948-9952; (c) Kang, P.; Cheng, C.; Chen, Z.; Schauer, C. K.; Meyer, T. J.; Brookhart, M. Selective Electrocatalytic Reduction of CO_2 to Formate by Water-Stable Iridium Dihydride Pincer Complexes. *J. Am. Chem. Soc.* **2012**, *134*, 5500-5503; (d) Zhang, Y.; MacIntosh, A. D.; Wong, J. L.; Bielinski, E. A.; Williard, P. G.; Mercado, B. Q.; Hazari, N.; Bernskoetter, W. H. Iron Catalyzed CO_2 Hydrogenation to Formate Enhanced by Lewis Acid Co-Catalysts. *Chem. Sci.* **2015**, *6*, 4291-4299; (e) Fei, H.; Sampson, M. D.; Lee, Y.; Kubiak, C. P.; Cohen, S. M. Photocatalytic CO_2 Reduction to Formate Using a Mn(I) Molecular Catalyst in a Robust Metal–Organic Framework. *Inorg. Chem.* **2015**, *54*, 6821-6828; (f) Hazari, N.; Heimann, J. E. Carbon Dioxide Insertion into Group 9 and 10 Metal–Element σ Bonds. *Inorg. Chem.* **2017**, *56*, 13655-13678; (g) Rønne, M. H.; Cho, D.; Madsen, M. R.; Jakobsen, J. B.; Eom, S.; Escoudé, É.; Hammershøj, H. C. D.; Nielsen, D. U.; Pedersen, S. U.; Baik, M.-H.; Skrydstrup, T.; Daasbjerg, K. Ligand-Controlled Product Selectivity in Electrochemical Carbon Dioxide Reduction Using Manganese Bipyridine Catalysts. *J. Am. Chem. Soc.* **2020**, *142*, 4265-4275.
13. By outer-sphere mechanism we mean that there is no interaction between the metal and CO_2 in the rate determining transition state. Instead the key interaction is between the nucleophilic hydride and the electrophilic carbon center of CO_2.
14. In the case of DMF and DMSO, which are the slowest solvents for CO_2 insertion, it was not possible to measure the rates of insertion into our full series of complexes because for some species with electron-withdrawing bpy substituents decomposition occurred on the same timescale as insertion.
15. Sullivan, B. P.; Meyer, T. J. Kinetics and Mechanism of Carbon Dioxide Insertion into a Metal-Hydride Bond. A Large Solvent Effect and an Inverse Kinetic Isotope Effect. *Organometallics* **1986**, *5*, 1500-1502.
16. (a) Heimann, J. E.; Bernskoetter, W. H.; Guthrie, J. A.; Hazari, N.; Mayer, J. M. Effect of Nucleophilicity on the Kinetics of CO_2 Insertion into Pincer-Supported Nickel Complexes. *Organometallics* **2018**, *37*, 3649-3653; (b) Deziel, A. P.; Espinosa, M. R.; Pavlovic, L.; Charboneau, D. J.; Hazari, N.; Hopmann, K. H.; Mercado, B. Q. Ligand and Solvent Effects on CO_2 Insertion into Group 10 Metal Alkyl Bonds. *Chem. Sci.* **2022**, *13*, 2391-2404.
17. Jaffé, H. H. A Reexamination of the Hammett Equation. *Chem. Rev.* **1953**, *53*, 191-261.
18. In this work, we used slightly different theoretical methods to those described in reference 11. As a consequence, the relative thermodynamic hydricities are slightly different from those we described previously. Intuitively, the thermodynamic hydricities calculated in this work are likely more precise, as in this case the trifluoromethyl substituted bpy complex is less thermodynamically hydridic than the methyl ether substituted bpy complex. For more information on the theoretical methods, see the SI.
19. Zhao, Y.; Truhlar, D. G. The M06 Suite of Density Functionals for Main Group Thermochemistry, Thermochemical Kinetics, Noncovalent Interactions, Excited States, and Transition Elements: Two New Functionals and Systematic Testing of Four M06-Class Functionals and 12 Other Functionals. *Theor. Chem. Acc.* **2008**, *120*, 215-241.
20. Marenich, A. V.; Cramer, C. J.; Truhlar, D. G. Universal Solvation Model Based on Solute Electron Density and on a Continuum Model of the Solvent Defined by the Bulk Dielectric Constant and Atomic Surface Tensions. *J. Phys. Chem. B* **2009**, *113*, 6378-6396.
21. (a) Lee, C.; Yang, W.; Parr, R. G. Development of the Colle-Salvetti Correlation-Energy Formula into a Functional of the Electron Density. *Phys. Rev. B* **1988**, *37*, 785; (b) Becke, A. D. Density-Functional Thermochemistry. III. The Role of Exact Exchange. *J. Chem. Phys.* **1993**, *98*, 5648-5652; (c) Grimme, S.; Ehrlich, S.; Goerigk, L. Effect of the Damping Function in Dispersion Corrected Density Functional Theory. *J. Comput. Chem.* **2011**, *32*, 1456-1465.

22. (a) Taheri, A.; Berben, L. A. Tailoring Electrocatalysts for Selective CO_2 or H^+ Reduction: Iron Carbonyl Clusters as a Case Study. *Inorg. Chem.* **2016**, *55*, 378-385; (b) Barlow, J. M.; Yang, J. Y. Thermodynamic Considerations for Optimizing Selective CO_2 Reduction by Molecular Catalysts. *ACS Cent. Sci.* **2019**, *5*, 580-588; (c) Ceballos, B. M.; Yang, J. Y. Highly Selective Electrocatalytic CO_2 Reduction by $[Pt(dmpe)_2]^{2+}$ Through Kinetic and Thermodynamic Control. *Organometallics* **2020**, *39*, 1491-1496.

TOC Graphic

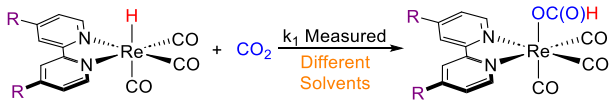

R = Electron donating or withdrawing

- Measured effect of solvent on kinetic and thermodynamic hydricity
- Derived LFERs between kinetic and thermodynamic hydricity in different solvents